

# New manganese(II) complexes with tetraorganodichalcogenoimidodiphosphinato ligands. Crystal and molecular structure of monomeric $\text{Mn}[(\text{SPMe}_2)(\text{SPh}_2)\text{N}]_2$ and dimeric $[\text{Mn}\{(\text{OPPh}_2)\{\text{OP}(\text{OEt})_2\}\text{N}\}_2(\text{H}_2\text{O})]_2$

Ana Maria Preda<sup>a</sup>, Anca Silvestru<sup>a,\*</sup>, Sorin Farcas<sup>b</sup>, Alina Bienko<sup>c</sup>, Jerzy Mrozinski<sup>c</sup>, Marius Andruh<sup>d</sup>

<sup>a</sup> Faculty of Chemistry and Chemical Engineering, "Babes-Bolyai" University, Cluj-Napoca RO-400028, Romania

<sup>b</sup> National Institute for Research and Development of Isotopic and Molecular Technologies, P.O. Box 700, Cluj-Napoca RO-400293, Romania

<sup>c</sup> Faculty of Chemistry, University of Wrocław, 14 F. Joliot-Curie, 50-383 Wrocław, Poland

<sup>d</sup> University of Bucharest, Faculty of Chemistry, Inorganic Chemistry Laboratory, Str. Dumbrova Rosie nr. 23, 020464 Bucharest, Romania

## ARTICLE INFO

### Article history:

Received 30 April 2008

Accepted 23 June 2008

Available online 31 July 2008

### Keywords:

Manganese(II) complexes

Molecular structure

Magnetic properties

## ABSTRACT

New manganese(II) complexes of type  $\text{Mn}[(\text{XPR}_2)(\text{YPR}'_2)\text{N}]_2$  [ $\text{X}, \text{Y} = \text{S}, \text{R} = \text{Me}, \text{R}' = \text{Ph}$  (**1**),  $\text{X} = \text{S}, \text{Y} = \text{O}, \text{R} = \text{Ph}, \text{R}' = \text{OEt}$  (**2**)] and  $\text{Mn}\{(\text{OPPh}_2)\{\text{OP}(\text{OEt})_2\}\text{N}\}_2(\text{H}_2\text{O})$  (**3**), were obtained by salt metathesis reactions between  $\text{MnCl}_2 \cdot 4\text{H}_2\text{O}$  and the potassium salts of the appropriate tetraorganodichalcogenoimidodiphosphinic acids. The complexes were characterized by EPR and IR spectroscopy, as well as by mass spectrometry. The crystal and molecular structures for **1** and **3** were determined by single-crystal X-ray diffraction. Compound **1** crystallizes as monomeric species, with the manganese(II) atom in a tetrahedral environment, while for compound **3** a dimeric structure was found. Both tetraorganodichalcogenoimidodiphosphinato ligand units behave monometallic biconnective in **1**, chelating the metal centre. In the dimeric species **3** the tetraphenylimidodiphosphinato ligand units behave different, two of them chelating the manganese atoms, as monometallic biconnective moieties, while the other two act bimetallic triconnective, bridging the two metal centres. The octahedral coordination geometry in **3** is completed by water molecules. The magnetic behaviour of **3** was investigated.

© 2008 Elsevier Ltd. All rights reserved.

## 1. Introduction

The coordination chemistry of the tetraorganodichalcogenoimidodiphosphinato ligands was extensively investigated, in connection both with Main Group or transition metals [1,2]. Complexes of the first row divalent metals, *i.e.* Mn(II), Fe(II), Co(II), Ni(II), with dithioimidodiphosphinato ligands exhibit mainly tetrahedral  $\text{MS}_4$  cores and the preference for a tetrahedral geometry versus a square planar one was assumed based on a low to medium ligand field strength of the  $[(\text{SPR}_2)_2\text{N}]^-$  ( $\text{R} = \text{Me}, \text{Ph}$ ) moiety [3].

The increased interest in manganese complexes is due mainly to their biological or magnetic properties. It was noticed the preference of manganese(II) for the hard O- or N-donor atoms in biological systems, in contrast with S-donor atoms [4,5]. On the other hand, magnetic materials are based on high-spin metal centres as manganese(II) or manganese(III) can generate with their five and four, respectively, unpaired electrons [6]. Even if it was observed that manganese containing proteins and magnetic materials are mainly based on ligands with oxygen as donor atoms, the

dithioato derivatives were also largely investigated. The manganese(II) derivatives of dithioato or diselenoato ligands form *spiro*-bicyclic monomeric structures with a slightly distorted tetrahedral  $\text{MnX}_4$  cores, as in the  $\text{Mn}[(\text{XPR}_2)(\text{YPR}'_2)\text{N}]_2$  species ( $\text{X} = \text{Y} = \text{S}, \text{R} = \text{R}' = \text{Ph}$  [7],  $\text{X} = \text{Y} = \text{S}, \text{R} = \text{R}' = \text{Pr}^i, \text{X} = \text{Y} = \text{S}, \text{R} = \text{Ph}, \text{R}' = \text{Pr}^i, \text{X} = \text{Y} = \text{Se}, \text{R} = \text{R}' = \text{Ph}$  [8]). For the monothio derivative  $\text{Mn}\{(\text{SPh}_2)(\text{OPPh}_2)\text{N}\}_2$  a similar monomeric structure was found [9], while for the dioxo analogue a dinuclear  $[\text{Mn}\{(\text{OPPh}_2)_2\text{N}\}_2]_2$  species was described [9,10]. For the manganese(I) compounds  $\text{Mn}(\text{CO})_4\{(\text{SPh}_2)_2\text{N}\}$  [11] and  $\text{Mn}_2(\text{CO})_6\{(\text{SPMe}_2)_2\text{N}\}_2$  [12], the tetraorganodithioimidodiphosphinato ligand exhibits either a monometallic biconnective or a bimetallic triconnective pattern, respectively, while for the manganese(III) derivative  $\text{Mn}\{(\text{OPPh}_2)_2\text{N}\}_3$  a monomeric structure with chelating ligands was reported [13].

As part of our studies on the influence of the nature of the chalcogen atoms and the organic groups in the ligand unit on the structure and properties of manganese complexes, we report here on the synthesis and spectroscopic characterization of some new manganese(II) derivatives of type  $\text{Mn}[(\text{XPR}_2)(\text{YPR}'_2)\text{N}]_2$  [ $\text{X}, \text{Y} = \text{S}, \text{R} = \text{Me}, \text{R}' = \text{Ph}$  (**1**),  $\text{X} = \text{S}, \text{Y} = \text{O}, \text{R} = \text{Ph}, \text{R}' = \text{OEt}$  (**2**)] and  $\text{Mn}\{(\text{OPPh}_2)\{\text{OP}(\text{OEt})_2\}\text{N}\}_2(\text{H}_2\text{O})$  (**3**), the molecular structures of **1** and **3**, as well as the magnetic behaviour of **3**.

\* Corresponding author. Tel.: +40 264 593833; fax: +40 264 590818.

E-mail address: [ancas@chem.ubbcluj.ro](mailto:ancas@chem.ubbcluj.ro) (A. Silvestru).

## 2. Experimental

Potassium tetraorganodichalcogenoimidodiphosphinates were prepared according to literature methods:  $K[(SPMe_2)(SPPH_2)N]$  [14],  $K[(SPPH_2)(OP(OEt)_2)N]$ ,  $K[(OPPh_2)(OP(OEt)_2)N]$  [15]. Solvents were purified by standard procedures and were freshly distilled prior to use. IR spectra were recorded in the range 4000–400  $cm^{-1}$  in KBr pellets on a Jasco FTIR-615 machine. Mass spectra were recorded on a FINNIGAN MAT 8200 instrument (CI). EPR spectra were recorded at 77 K and at room temperature on a Bruker ESP 300 spectrometer operating in X-band, equipped with an ER 035 M Bruker NMR gaussmeter and a HP 3530B Hewlett-Packard microwave frequency counter, and only at room temperature on a X-band Radiopan SE/X 2543 Spectrometer, respectively. All  $g$  factors were determined with  $\pm 0.05$  accuracy. Magnetic measurements in the temperature range of 1.8–300 K were carried out on powdered samples of complex **3**, at a magnetic field of 0.5 T and at 2 K in the range of 0–5 T, using a Quantum Design SQUID based MPMSXL-5 type magnetometer. Corrections are based on subtracting the sample-holder signal and the contribution  $\chi_D = 1181 \times 10^{-6} cm^3 mol^{-1}$  was estimated from the Pascal constants [16]. Elemental analyses were performed on a VarioEL analyzer.

### 2.1. Preparation of bis[*P,P*-dimethyl-*P,P'*-diphenyl-dithioimido-diphosphinato]manganese(II), $Mn[(SPMe_2)(SPPH_2)N]_2$ (**1**)

A reaction mixture of  $K[(SPMe_2)(SPPH_2)N]$  (0.515 g, 1.420 mmol) and  $MnCl_2 \cdot 4H_2O$  (0.140 g, 0.707 mmol) in methanol (50 ml) was stirred at room temperature for 24 h. The solvent was completely removed in vacuum and the remaining solid was extracted with toluene. The clear solution was concentrated in vacuum, yielding the title compound as a colourless crystalline product. Yield: 0.261 g (52%), m.p. 119–120 °C. *Anal. Calc.* for  $C_{28}H_{32}MnN_2P_4S_4$ : C, 47.79; H, 4.58; N, 3.98. Found: C, 47.68; H, 4.52; N, 3.97%. IR ( $cm^{-1}$ ): 1197s, br [ $\nu_{as}(P_2N)$ ], 589s [ $\nu(PhPS)$ ], 571s [ $\nu(MePS)$ ].  $Cl_{pos}$  MS ( $m/z$ , %): 703 (42) [ $M^+$ ], 324 (100) [ $[(SPMe_2)(SPPH_2)N]^+$ ].  $Cl_{neg}$  MS ( $m/z$ , %): 703 (18) [ $M^-$ ], 324 (57) [ $[(SPMe_2)(SPPH_2)N]^-$ ], 110 (100) [ $(SPMe_2 + NH_3)^-$ ].

Compounds **2** and **3** were similarly prepared:

*Bis[*P,P*-diethoxy-*P,P'*-diphenyl-*P*-thioimidodiphosphinato]manganese(II)*,  $Mn[(SPPH_2)(OP(OEt)_2)N]_2$  (**2**) from  $K[(SPPH_2)(OP(OEt)_2)N]$  (0.720 g, 1.769 mmol) and  $MnCl_2 \cdot 4H_2O$  (0.175 g, 0.883 mmol). Yield: 0.315 g (45%), m.p. 95 °C. *Anal. Calc.* for  $C_{32}H_{40}MnN_2O_6S_2P_4$ : C, 48.55; H, 5.09; N, 3.54. Found: C, 48.61; H, 5.05; N, 3.55%. IR ( $cm^{-1}$ ): 1265vs [ $\nu_{as}(P_2N)$ ], 1104s [ $\nu(PO)$ ], 1033vs, br [ $\nu(POC)$ ], 599s [ $\nu(PS)$ ].  $Cl_{pos}$  MS ( $m/z$ , %): 792 (100) [ $(M+H)^+$ ], 370 (92) [ $[(SPPH_2)(OP(OEt)_2)NH]^+$ ].  $Cl_{neg}$  MS ( $m/z$ , %): 792 (12) [ $(M+H)^-$ ], 368 (100) [ $[(SPPH_2)(OP(OEt)_2)N]^-$ ], 336 (26) [ $[(PPH_2)(OP(OEt)_2)N]^-$ ].

*Bis[*P,P*-diethoxy-*P,P'*-diphenyl-imidodiphosphinato]manganese(II) water solvate*,  $Mn[(OPPh_2)(OP(OEt)_2)N]_2(H_2O)$  (**3**) from  $K[(OPPh_2)(OP(OEt)_2)N]$  (0.151 g, 1.317 mmol) and  $MnCl_2 \cdot 4H_2O$  (0.130 g, 0.658 mmol). Yield: 0.36 g (70%), m.p. 100–102 °C. *Anal. Calc.* for  $C_{32}H_{42}MnN_2O_9P_4$ : C, 49.43; H, 5.44; N, 3.60. Found: C, 49.75; H, 5.18; N, 3.65%. IR ( $cm^{-1}$ ): 1244vs [ $\nu_{as}(P_2N)$ ], 1157vs, 1143vs [ $\nu(PO)$ ], 1067vs, 1041vs [ $\nu(POC)$ ].  $Cl_{pos}$  MS ( $m/z$ , %): 759 (52) [ $[Mn\{(OPPh_2)(OP(OEt)_2)N\}_2]^+$ ], 353 (100) [ $[(OPPh_2)(OP(OEt)_2)NH]^+$ ].  $Cl_{neg}$  MS ( $m/z$ , %): 760 (12) [ $[Mn\{(OPPh_2)(OP(OEt)_2)N\}_2+H]^+$ ], 352 (100) [ $[(OPPh_2)(OP(OEt)_2)N]^-$ ], 336 (26) [ $[(PPH_2)(OP(OEt)_2)N]^-$ ].

## 3. Crystal structure determination

Colourless block crystals of  $Mn[(SPMe_2)(SPPH_2)N]_2$  (**1**) and  $Mn[(OPPh_2)(OP(OEt)_2)N]_2(H_2O)$  (**3**) were attached with epoxy glue

**Table 1**

Crystal data and structure refinement for  $Mn[(SPMe_2)(SPPH_2)N]_2$  (**1**) and  $Mn[(OPPh_2)(OP(OEt)_2)N]_2(H_2O)$  (**3**)

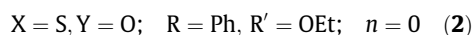
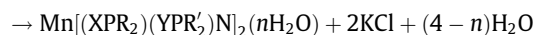
	<b>1</b>	<b>3</b>
Empirical formula	$C_{28}H_{32}MnN_2P_4S_4$	$C_{64}H_{84}Mn_2N_4O_{18}P_8$
Formula weight	703.62	1554.99
Temperature (K)	297(2)	297(2)
Wavelength (Å)	0.71073	0.71073
Crystal system	monoclinic	triclinic
Space group	$P2(1)/c$	$P2(1)/n$
$a$ (Å)	15.0259(11)	11.9760(9)
$b$ (Å)	11.9642(9)	13.5226(10)
$c$ (Å)	19.1422(14)	13.6310(11)
$\alpha$ (°)	90	108.6870(10)
$\beta$ (°)	106.0830(10)	106.4710(10)
$\gamma$ (°)	90	97.7490(10)
Volume (Å <sup>3</sup> )	3306.6(4)	1942.4(3)
$Z$	4	1
$D_{calc}$ (g/cm <sup>3</sup> )	1.413	1.329
Absorption coefficient (mm <sup>-1</sup> )	0.867	0.555
$F(000)$	1452	810
Crystal size (mm)	0.29 × 0.23 × 0.21	0.30 × 0.29 × 0.22
$\theta$ Range for data collections (°)	2.03 to 25.00	1.68 to 26.37
Reflections collected	23505	20991
Independent reflections ( $R(int)$ )	5835 (0.0497)	7887 (0.0413)
Maximum and minimum transmissions	0.8388 and 0.7871	0.8877 and 0.8513
Refinement method	Full-matrix least-squares on $F^2$	
Data/restraints/parameters	5835/0/356	7887/0/456
Goodness-of-fit on $F^2$	1.154	1.146
Final $R$ indices [ $I > 2\sigma(I)$ ]	$R_1 = 0.0560$ , $wR_2 = 0.1206$	$R_1 = 0.0667$ , $wR_2 = 0.1424$
$R$ indices (all data)	$R_1 = 0.0692$ , $wR_2 = 0.1261$	$R_1 = 0.0881$ , $wR_2 = 0.1525$
Largest difference in peak and hole (eÅ <sup>-3</sup> )	0.458 and -0.238	0.573 and -0.271

on cryoloops. The data were collected on a Bruker SMART APEX CCD diffractometer using graphite-monochromated  $Mo K\alpha$  radiation ( $\lambda = 0.71073$  Å). Data reduction was performed using the SAINT-PLUS software and the data were corrected for absorption effects using the SADABS program [17]. The details of the crystal structure determination and refinement are given in Table 1.

Cell refinement gave cell constants corresponding to monoclinic (**1**) and triclinic (**3**) cells. The structures were solved by direct methods [18] and refined using the SHELXTL [19] version of SHELX-97 [20]. Compound **3** is centrosymmetric with an inversion centre in the middle of the  $Mn_2O_2$  ring and thus half of the molecule is generated by symmetry. The hydrogen atoms were refined with a riding model and a mutual isotropic thermal parameter, excepting the hydrogen atoms from the water molecule in **3**, which were located on the difference map and refined at a O–H distance of 0.82(5) and 0.80(5) Å, respectively. C16 in **3** is disordered and was refined over two positions with 49% and 51% occupancy. The drawings were created with the DIAMOND program [21].

## 4. Results and discussion

Manganese(II) complexes were obtained in moderate yields by salt metathesis reactions between  $MnCl_2 \cdot 4H_2O$  and the potassium salt of the appropriate tetraorganodichalcogenoimidodiphosphinic acid, in a 1:2 molar ratio.



The complexes were isolated as colourless (**1** and **3**) or slight pink (**2**) solids and were characterized by mass spectrometry, IR and EPR spectroscopy. For compounds **1** and **3** the crystal and molecular structure was determined by single-crystal X-ray diffraction.

In the CI mass spectra of the title compounds either the molecular or the pseudo-molecular ions appear with high or medium intensity, i.e.  $[\text{Mn}\{(\text{SPPPh}_2)(\text{SPMe}_2)\text{N}\}_2]^+$  ( $m/z$  703, 42%),  $[\text{Mn}\{(\text{SPPPh}_2)\{\text{OP}(\text{OEt})_2\text{N}\}_2 + \text{H}\}]^+$  ( $m/z$  792, 100%) and  $[\text{Mn}\{(\text{OPPh}_2)\{\text{OP}(\text{OEt})_2\text{N}\}_2\}]^+$  ( $m/z$  759, 52%) for **1**, **2** and **3**, respectively. For derivative **3** the dimeric species or fragments with a higher mass than that corresponding to the monomeric species were not observed by chemical ionization.

The IR spectra are consistent with the coordination of the ligand units in the deprotonated form, through both chalcogen atoms. The strong absorption bands observed for the Mn(II) complexes in the ranges 1250–1200, 1150–1110 and 600–550  $\text{cm}^{-1}$  were assigned to  $\nu_{\text{as}}(\text{P}_2\text{N})$ ,  $\nu(\text{PO})$  and  $\nu(\text{PS})$  stretching vibrations, respectively, in comparison with the potassium salts used as starting materials [14,15].

The EPR spectra of the manganese(II) complexes are expected to display a fine structure of five lines. However, only for compounds **2** and **3** the fine structure was observed, while for the derivative **1** only a broad band was found at room temperature ( $g = 1.94$ ), due probably to the paramagnetic ion clusters present in this sample. The line width (390 Gs for **1**, 502 Gs and 400 Gs for the central line of **2** and **3**, respectively) is consistent with a strong crystal field around the paramagnetic ions. This behaviour might be explained by the strong interaction with the crystal field created by the ligands and the covalent interactions between the Mn(II) ion and the ligands. The  $g$  values determined at room temperature for the compounds **2** and **3** (2.01 and 2.03, respectively) are also consistent with strong covalent interactions. Theoretical calculations allowed us to determine the crystal field constant  $D$  (431 Gs) for the species **3**, which exhibits a fine structure. In the case of this polycrystalline material we average the  $\theta$  angle between the direction of the magnetic induction and the symmetry axes of the magnetic centre from 0 to  $\pi/2$  in the Spin Hamiltonian [22].

The EPR spectrum of the complex **3** at 4.2 K exhibits a single broad line with  $g = 1.98$ ,  $\Delta H_{\text{pp}} = 565$  Gs ( $\Delta H_{\text{pp}} =$  peak to peak line-width) and shows a partial resolved hyperfine structure due to the interaction between the transition inside Kramer's doublet ( $\pm 1/2$ ) and the  $^{55}\text{Mn}(\text{II})$  nuclear spin  $I = 5/2$ , of a value about 95 Gs (Fig. 1).

#### 4.1. Crystal and molecular structure of $\text{Mn}\{(\text{SPMe}_2)(\text{SPPPh}_2)\text{N}\}_2$ (**1**)

The molecular structure of **1** was determined by single-crystal X-ray diffraction. Important bond distances and angles are listed in Table 2.

The crystal of **1** consists of distinct monomeric units separated by normal van der Waals distances. An ORTEP-like diagram with the atom numbering scheme is given in Fig. 2.

The dithioato ligand units behave monometallic biconnective, resulting in a *spiro*-bicyclic system with a slightly distorted tetrahedral  $\text{MnS}_4$  core (S–Mn–S bond angles in the range 106.3–113.9°). One of the endocyclic angles is larger [S(3)–Mn(1)–S(4) 111.02(4)°], while the other one [S(1)–Mn(1)–S(2) 109.32(4)°] is close to the tetrahedral value of 109.5°. The dihedral angle between the S(1)/Mn(1)/S(2) and S(3)/Mn(1)/S(4) planes is 87.46(4)°, larger than those observed for  $\text{Mn}\{(\text{SPPPh}_2)_2\text{N}\}_2$  (86.8°) [7] and  $\text{Mn}\{(\text{SPPPh}_2)(\text{SPPPh}_2)\text{N}\}_2$  [78.99(3)°] [8], and slightly smaller than that one found for  $\text{Mn}\{(\text{SPPPh}_2)_2\text{N}\}_2$  [88.12(1)°] [8]. The Mn–S bond distances [av. 2.423(1) Å] are similar to those found in  $\text{Mn}\{(\text{SPPPh}_2)_2\text{N}\}_2$  [av. 2.443(12) Å] [7].

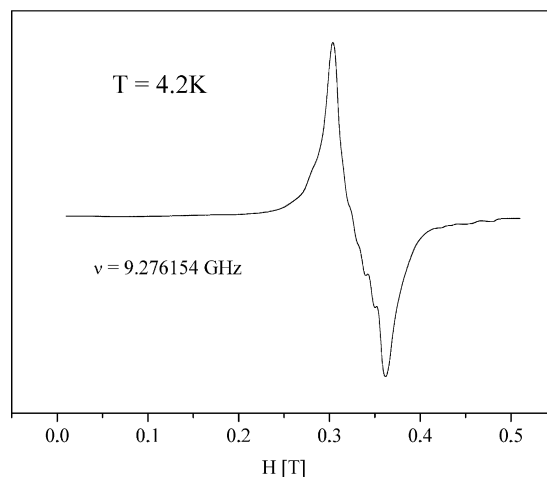


Fig. 1. EPR spectrum of **3** at 4.2 K.

Table 2

Selected interatomic distances (Å) and angles (°) in  $\text{Mn}\{(\text{SPPPh}_2)(\text{SPMe}_2)\text{N}\}_2$  (**1**)

Mn(1)–S(1)	2.4354(12)	Mn(1)–S(3)	2.4438(12)
Mn(1)–S(2)	2.4136(12)	Mn(1)–S(4)	2.4001(12)
S(1)–P(1)	2.0159(14)	S(3)–P(3)	2.0177(14)
S(2)–P(2)	2.0213(14)	S(4)–P(4)	2.0155(15)
N(1)–P(1)	1.595(3)	N(2)–P(3)	1.582(3)
N(1)–P(2)	1.591(3)	N(2)–P(4)	1.591(3)
S(1)–Mn(1)–S(2)	109.31(4)	S(3)–Mn(1)–S(4)	111.02(4)
S(1)–Mn(1)–S(3)	113.90(4)	S(2)–Mn(1)–S(4)	108.11(4)
S(1)–Mn(1)–S(4)	106.33(4)	S(2)–Mn(1)–S(3)	108.02(4)
Mn(1)–S(1)–P(1)	105.10(5)	Mn(1)–S(3)–P(3)	104.70(5)
Mn(1)–S(2)–P(2)	99.59(5)	Mn(1)–S(4)–P(4)	99.63(5)
N(1)–P(1)–S(1)	118.68(12)	N(2)–P(3)–S(3)	118.53(12)
N(1)–P(2)–S(2)	115.90(12)	N(2)–P(4)–S(4)	118.27(13)
P(1)–N(1)–P(2)	129.5(2)	P(3)–N(2)–P(4)	134.7(2)

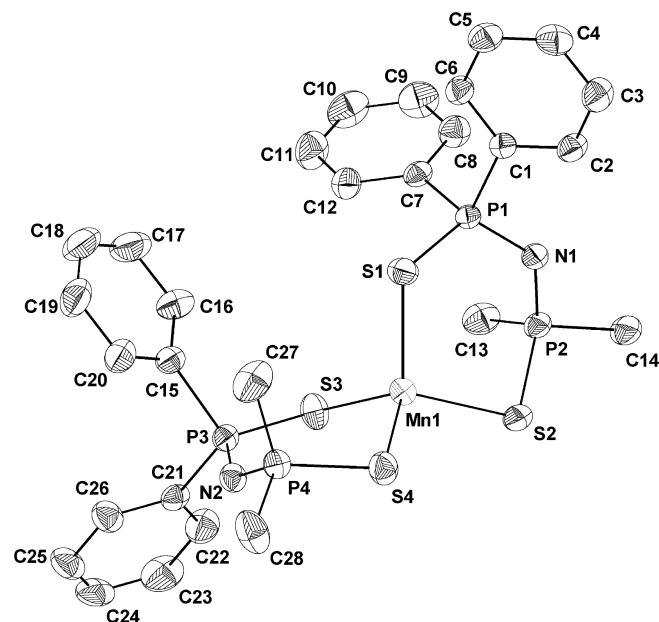


Fig. 2. ORTEP plot at 40% probability and atom numbering scheme for **1**. For clarity, the hydrogen atoms are omitted.

The two six-membered  $\text{MnS}_2\text{P}_2\text{N}$  chelate rings are not planar and display twisted chair conformations with the  $\text{Mn}(1)/\text{N}(1)$  and  $\text{Mn}(1)/\text{N}(2)$  atoms, respectively, in apices. In contrast, twisted boat conformations were observed for other reported dithioato derivatives, *i.e.*  $\text{Mn}[(\text{SPPPh}_2)_2\text{N}]_2$  [7] and  $\text{Mn}[(\text{SPPPr}_2)_2\text{N}]_2$  [8] (with phosphorus and sulfur atoms in the apices) or  $\text{Mn}[(\text{SPPPr}_2)(\text{SPPPh}_2)\text{N}]_2$  [8] (with manganese and nitrogen atoms in apices), respectively.

The phosphorus–sulfur [range of 2.0155(15)–2.0213(14) Å] and phosphorus–nitrogen [range of 1.582(3)–1.595(3) Å] distances, respectively, are intermediate between the single and the double bonds [cf.  $\text{Ph}_2\text{P}(\text{=S})\text{N}=\text{P}(\text{SMe})\text{Ph}_2$  [23]:  $\text{P}=\text{S}$  1.954(1) Å,  $\text{P}-\text{S}$

2.071(1) Å,  $\text{P}=\text{N}$  1.562(2) Å,  $\text{P}-\text{N}$  1.610(2) Å]. The  $\text{P}-\text{N}-\text{P}$  angles are different in the two ligand moieties [ $\text{P}(1)-\text{N}(1)-\text{P}(2)$  129.5(2) and  $\text{P}(3)-\text{N}(2)-\text{P}(4)$  134.7(2)°], both being considerably larger in comparison with the free acid [ $\text{P}-\text{N}-\text{P}$  126.1(4)°] [24], and thus suitable to accommodate around the metal centre.

#### 4.2. Crystal and molecular structure of $\text{Mn}[(\text{OPPh}_2)\{\text{OP}(\text{OEt})_2\text{N}\}_2(\text{H}_2\text{O})]$ (**3**)

Selected bond distances and angles for **3** are listed in Table 3 and the ORTEP-like diagram with the atom numbering scheme is given in Fig. 3.

The crystal contains discrete dimer associations in which the metal centres are bridged by the oxygen atoms of the  $\text{OP}(\text{OEt})_2$  groups from two ligand units acting as bimetallic triconnective moieties, thus resulting in a fused tricyclic  $\text{Mn}_2\text{O}_4\text{P}_4\text{N}_2$  system. The other two ligands chelate each a metal atom, resulting in an overall structure which resembles that found in the dimeric  $[\text{Mn}\{(\text{OPPh}_2)_2\text{N}\}_2]_2$  [9]. However some significant differences have to be noted. The central four-membered  $\text{Mn}_2\text{O}_2$  ring in the dimer of the title compound **3** is planar, while it is slightly folded in the related  $[\text{Mn}\{(\text{OPPh}_2)_2\text{N}\}_2]_2$ . This behaviour is consistent with a larger nonbonding  $\text{Mn}\cdots\text{Mn}$  distance in **3** than in  $[\text{Mn}\{(\text{OPPh}_2)_2\text{N}\}_2]_2$  [3.4073(6) Å versus 3.378(3) Å].

The overall conformation of the  $[\text{Mn}\{(\text{OPPh}_2)_2\text{N}\}_2]_2$  dimer might be described as *cis*, *i.e.* with the six-membered  $\text{MnO}_2\text{P}_2\text{N}$  rings formed by ligands of the same type placed on the same side of the four-membered  $\text{Mn}_2\text{O}_2$  ring (Fig. 4 a) [9]. By contrast, the fused tricyclic  $\text{Mn}_2\text{O}_4\text{P}_4\text{N}_2$  system in the dimer of **3** is considerably flattened, with equivalent atoms of the six-membered  $\text{MnO}_2\text{P}_2\text{N}$  rings deviated on opposite sides of the central planar  $\text{Mn}_2\text{O}_2$  core [deviations from  $\text{Mn}_2\text{O}_2$  plane:  $\text{O}(3)$  0.042,  $\text{P}(3)$  0.226,  $\text{N}(2)$  –0.160 Å, and  $\text{P}(4)$  0.419 Å, respectively]. The chelate  $\text{MnO}_2\text{P}_2\text{N}$  rings are placed on opposite sides of this flattened tricyclic system and the overall conformation in the dimer of **3** might be described as *trans* (Fig. 4 b).

The oxygen atom from a water molecule completes a distorted octahedral coordination geometry around the manganese atoms in the dimer of **3**, in contrast with the trigonal bipyramidal geometry observed for the related  $[\text{Mn}\{(\text{OPPh}_2)_2\text{N}\}_2]_2$  analogue [9]. Moreover, the water molecules are involved in hydrogen bonding with

**Table 3**

Selected interatomic distances (Å) and angles (°) in  $\text{Mn}[(\text{OPPh}_2)\{\text{OP}(\text{OEt})_2\text{N}\}_2(\text{H}_2\text{O})]$  (**3**)<sup>a</sup>

$\text{Mn}(1)-\text{O}(1)$	2.088(2)	$\text{Mn}(1)-\text{O}(3)$	2.102(2)
$\text{Mn}(1)-\text{O}(2)$	2.168(2)	$\text{Mn}(1)-\text{O}(4)$	2.237(2)
		$\text{Mn}(1)-\text{O}(4a)$	2.247(2)
$\text{Mn}(1)-\text{O}(9)$	2.271(3)		
$\text{O}(1)-\text{P}(1)$	1.508(2)	$\text{O}(3)-\text{P}(3)$	1.500(3)
$\text{O}(2)-\text{P}(2)$	1.496(2)	$\text{O}(4)-\text{P}(4)$	1.503(2)
$\text{O}(5)-\text{P}(2)$	1.572(3)	$\text{O}(7)-\text{P}(5)$	1.556(3)
$\text{O}(6)-\text{P}(2)$	1.573(3)	$\text{O}(8)-\text{P}(5)$	1.577(3)
$\text{N}(1)-\text{P}(1)$	1.595(3)	$\text{N}(2)-\text{P}(3)$	1.587(3)
$\text{N}(1)-\text{P}(2)$	1.553(3)	$\text{N}(2)-\text{P}(4)$	1.567(3)
$\text{O}(1)-\text{Mn}(1)-\text{O}(4)$	174.98(9)	$\text{O}(3)-\text{Mn}(1)-\text{O}(4a)$	169.96(9)
$\text{O}(2)-\text{Mn}(1)-\text{O}(9)$	163.68(10)		
$\text{O}(1)-\text{Mn}(1)-\text{O}(2)$	93.52(9)	$\text{O}(4)-\text{Mn}(1)-\text{O}(2)$	91.15(9)
$\text{O}(1)-\text{Mn}(1)-\text{O}(3)$	92.32(9)	$\text{O}(4)-\text{Mn}(1)-\text{O}(3)$	88.92(9)
$\text{O}(1)-\text{Mn}(1)-\text{O}(9)$	93.73(11)	$\text{O}(4)-\text{Mn}(1)-\text{O}(9)$	81.29(11)
$\text{O}(1)-\text{Mn}(1)-\text{O}(4a)$	97.51(9)	$\text{O}(4)-\text{Mn}(1)-\text{O}(4a)$	81.11(9)
$\text{O}(2)-\text{Mn}(1)-\text{O}(3)$	97.16(10)	$\text{O}(9)-\text{Mn}(1)-\text{O}(4a)$	80.26(10)
$\text{O}(3)-\text{Mn}(1)-\text{O}(9)$	97.13(11)	$\text{O}(4a)-\text{Mn}(1)-\text{O}(2)$	84.31(9)
$\text{Mn}(1)-\text{O}(4)-\text{Mn}(1a)$	98.89(9)		
$\text{Mn}(1a)-\text{O}(4)-\text{P}(4)$	125.07(13)	$\text{Mn}(1)-\text{O}(3)-\text{P}(3)$	131.25(15)
$\text{Mn}(1)-\text{O}(2)-\text{P}(2)$	127.83(13)	$\text{Mn}(1)-\text{O}(4)-\text{P}(4)$	126.95(14)
		$\text{Mn}(1a)-\text{O}(4)-\text{P}(4)$	130.33(13)
$\text{O}(1)-\text{P}(1)-\text{N}(1)$	119.60(15)	$\text{O}(3)-\text{P}(3)-\text{N}(2)$	118.24(15)
$\text{O}(2)-\text{P}(2)-\text{N}(1)$	117.87(15)	$\text{O}(4)-\text{P}(4)-\text{N}(2)$	117.29(15)
$\text{P}(1)-\text{N}(1)-\text{P}(2)$	130.2(2)	$\text{P}(3)-\text{N}(2)-\text{P}(4)$	128.2(2)

<sup>a</sup> Symmetry equivalent positions ( $-x$ ,  $-y$ ,  $-z$ ) are given by "a".

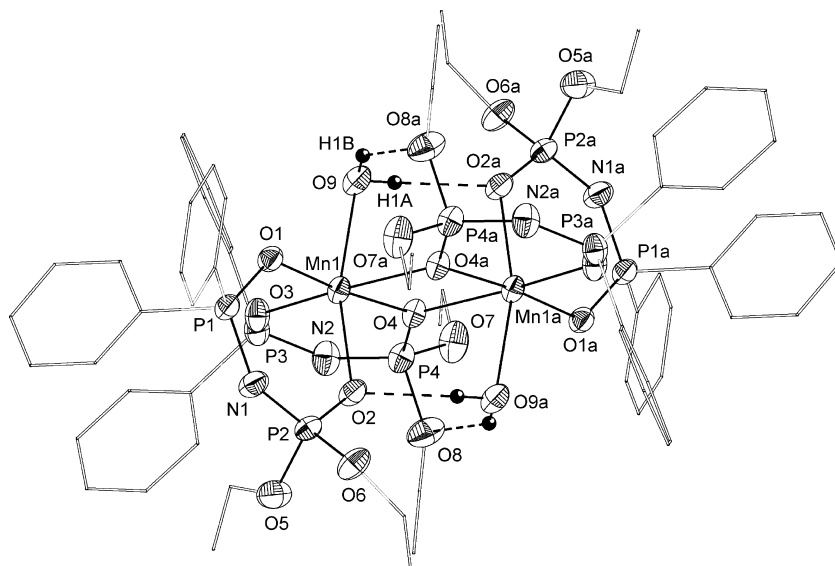


**Fig. 3.** ORTEP plot of the dimer unit in the crystal of **3**. The atoms are drawn with 30% probability ellipsoids [symmetry equivalent atoms ( $-x$ ,  $-y$ ,  $-z$ ) are given by "a"]. For clarity, the hydrogen atoms, other than water hydrogens, are omitted.

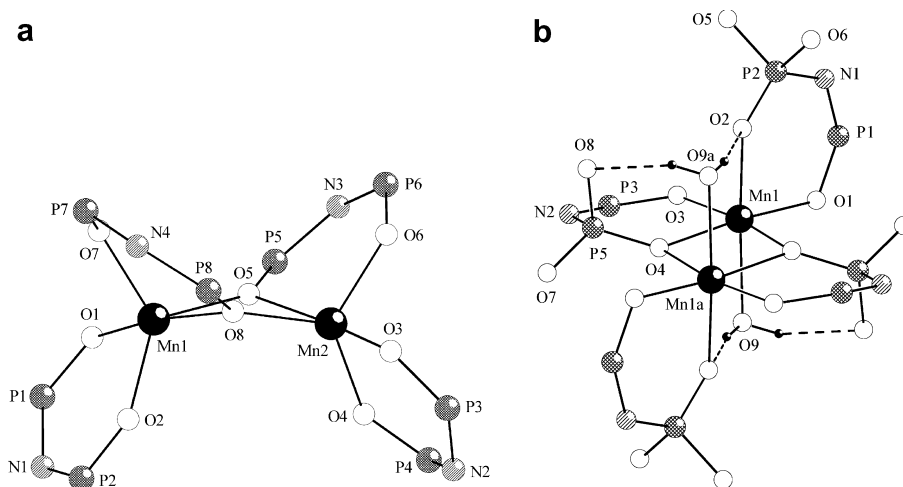


Fig. 4. Dimer cores in (a)  $[\text{Mn}((\text{OPPh}_2)_2\text{N})_2]_2$  [9], and (b) title compound **3**. For clarity, the hydrogen atoms, other than water hydrogens, and the carbon atoms are omitted.

the oxygen atom connected to the metal centre from the chelating ligand  $[\text{H}(1\text{A})\cdots\text{O}(2\text{a})$  2.05 Å) and one oxygen atom of an ethoxy group from the bridging ligand  $[\text{H}(1\text{B})\cdots\text{O}(8\text{a})$  2.30 Å], respectively (Fig. 3).

The monometallic biconnective  $\text{MnO}_2\text{P}_2\text{N}$  rings show distorted chair conformations with nitrogen and manganese atoms in apices, while for the bridging ligands the corresponding  $\text{MnO}_2\text{P}_2\text{N}$  rings exhibit distorted boat conformations, with bridging O(4) and P(3) atoms in apices.

The Mn–O distances in the Mn–O–Mn bridge are equivalent [Mn(1)–O(4) 2.237(2), Mn(1)–O(4a) 2.247(2) Å] and considerably longer than the Mn(1)–O(3) bond distance [2.102(2) Å] in the same ligand unit. Even longer is the Mn–O<sub>water</sub> bond distance [Mn(1)–O(9) 2.271(3) Å]. For the monometallic biconnective ligand moiety the Mn–O bonds are also not equivalent [Mn(1)–O(1) 2.088(2), Mn(1)–O(2) 2.168(2) Å], a behaviour which contrasts with that observed for the ligand moieties exhibiting a similar, but symmetric, coordination pattern in the related  $[\text{Mn}\{(\text{OPPh}_2)_2\text{N}\}_2]_2$  dimer [9].

The phosphorus–nitrogen [range 1.553(3)–1.595(3) Å] and phosphorus–oxygen distances [range 1.496(2)–1.508(2) Å], respectively, are of a magnitude intermediate between a single and a double bond, thus suggesting some delocalization of the  $\pi$  electrons on the OPNPO system in all four ligand units (cf.  $[(\text{Me}_3\text{Si})_2\text{N}-\text{P}(=\text{N}^t\text{Bu})\text{S}]_2$  [25]: P=N 1.529(2) Å, P–N 1.662(2) Å;  $\text{Ph}_2\text{P}(\text{O})\text{OH}$  [26]: P=O 1.486(6) Å, P–O 1.526(6) Å).

### 4.3. Magnetic properties

The magnetic behaviour of complex **3** in the form of  $\chi_{\text{Mn}}T$  versus  $T$  curve is shown in Fig. 5 ( $\chi_{\text{Mn}}$  is the molar magnetic susceptibility per Mn(II) ion). The value of  $\chi_{\text{Mn}}T$  product at room temperature is 4.87  $\text{cm}^3 \text{mol}^{-1} \text{K}$  ( $\mu_{\text{eff.}} = 6.24$  B.M.), which is slightly larger than that calculated for  $S = 5/2$  with  $g = 2$  (4.375  $\text{cm}^3 \text{mol}^{-1} \text{K}$ ,  $\mu_{\text{eff.}} = 5.92$  B.M.). Upon lowering the temperature,  $\chi_{\text{Mn}}T$  decreases gradually and reaches a value of 0.61  $\text{cm}^3 \text{mol}^{-1} \text{K}$  at 1.8 K.

The temperature variation of  $\chi_{\text{Mn}}^{-1}$ , from room temperature down to 10 K, follows a Curie–Weiss law ( $\chi_{\text{Mn}} = C/(T - \Theta)$ ), with  $C = 5.36 \text{ cm}^3 \text{mol}^{-1} \text{K}$  and  $\Theta = -28.9$  K. Below 10 K, the slope of  $\chi_{\text{Mn}}^{-1}$  changes (inset to Fig. 5). The magnetic susceptibility can be analyzed using the isotropic spin Hamiltonian:  $H = -2J\hat{S}_1\hat{S}_2$ . The temperature dependence of the magnetic susceptibility is given by the equation [27]:

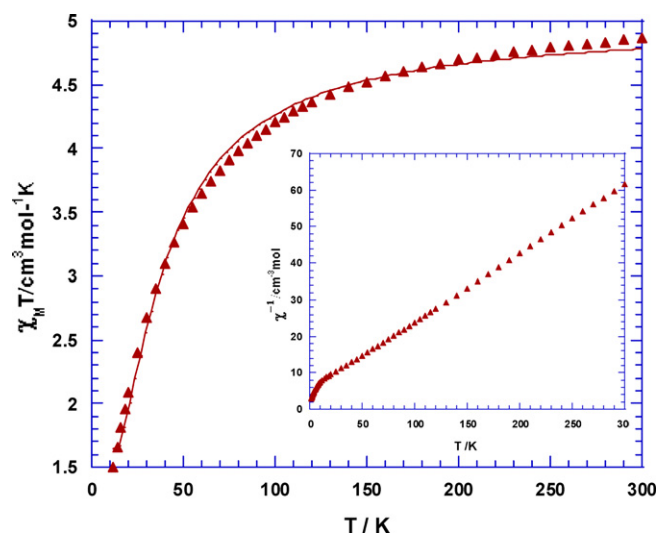


Fig. 5. Plot of  $\chi_{\text{Mn}}T$  vs.  $T$  in the temperature range 10–300 K for **3**. The solid line represents the best fit to the experimental data with the parameters reported in the text (inset: temperature dependence of  $\chi_{\text{Mn}}^{-1}$ ).

$$\chi_{\text{Mn}} = \frac{Ng^2\beta^2}{kT} \frac{55 + 30e^{5x} + 14e^{9x} + 5e^{12x} + e^{14x}}{11 + 9e^{5x} + 7e^{9x} + 5e^{12x} + 3e^{14x} + e^{15x}}, \quad x = \frac{-2J}{kT}$$

Additional interdimer interactions have been introduced in the frame of the mean-field approximation [28]:

$$\chi_{\text{Mn}}^{\text{corr}} = \frac{\chi_{\text{Mn}}}{1 - \frac{2zJ'}{N\beta^2g^2} \chi_{\text{Mn}}}$$

$zJ'$  is the intermolecular exchange parameter and  $z$  is the number of the nearest neighbours. Least-square fit to the experimental data gives  $J = -3.5 \text{ cm}^{-1}$ ,  $zJ' = -1.0 \text{ cm}^{-1}$ ,  $g = 1.99$ .

### 5. Supplementary data

CCDC 656244 and 656245 contain the supplementary crystallographic data for **1** and **3**. These data can be obtained free of charge via <http://www.ccdc.cam.ac.uk/conts/retrieving.html>, or from the Cambridge Crystallographic Data Centre, 12 Union Road, Cambridge CB2 1EZ, UK; fax: (+44) 1223-336-033; or e-mail: deposit@ccdc.cam.ac.uk.

## Acknowledgements

This work was supported by the Romanian Ministry of Education and Research (Grant CERES 4-62/2004) and the Polish Ministry of Science and Higher Education (Grant No. 1T09A 12430).

## References

- [1] J.D. Woollins, *J. Chem. Soc., Dalton Trans.* (1996) 2893.
- [2] C. Silvestru, J.E. Drake, *Coord. Chem. Rev.* 223 (2001) 117.
- [3] O. Siiman, *Inorg. Chem.* 20 (1981) 2285 and references cited therein.
- [4] J.J.R.F. da Silva, R.J.P. Williams, *The Biological Chemistry of the Elements*, second ed., Oxford University Press, 2001 (Chapter 14).
- [5] U. Bossek, H. Hummel, T. Weyhermueller, K. Wieghardt, S. Russell, L. van der Wolf, U. Kolb, *Angew. Chem., Int. Ed. Engl.* 35 (1996) 1552. and references cited therein.
- [6] J.D. Martin, R.F. Hess, *Chem. Commun.* (1996) 2419.
- [7] O. Siiman, H.B. Gray, *Inorg. Chem.* 13 (1974) 1185.
- [8] D. Maganas, S.S. Staniland, A. Grigoropoulos, F. White, S. Parsons, N. Robertson, P. Kyritsis, G. Pneumatikakis, *Dalton Trans.* (2006) 2301.
- [9] I. Szekeley, C. Silvestru, J.E. Drake, G. Balazs, S.I. Farcas, I. Haiduc, *Inorg. Chim. Acta* 299 (2000) 247.
- [10] I. Szekeley, J.E. Drake, C. Silvestru, *Phosphorus, Sulfur and Silicon* 124 and 125 (1997) 557.
- [11] N. Zuniga-Villarreal, C. Silvestru, M. Reyes-Lezama, S. Hernandez-Ortega, C. Alvarez Toledano, *J. Organomet. Chem.* 496 (1995) 169.
- [12] N. Zuniga-Villarreal, M. Reyes-Lezama, G. Espinosa, *J. Organomet. Chem.* 626 (2001) 113.
- [13] N. Zuniga-Villarreal, M. Reyes-Lezama, S. Hernandez-Ortega, C. Silvestru, *Polyhedron* 17 (1998) 2679.
- [14] R. Roesler, C. Silvestru, G. Espinosa-Perez, I. Haiduc, R. Cea-Olivares, *Inorg. Chim. Acta* 241 (1996) 47.
- [15] G. Balazs, J.E. Drake, C. Silvestru, I. Haiduc, *Inorg. Chim. Acta* 287 (1999) 61.
- [16] E. König, *Magnetic Properties of Coordination and Organometallic Transition Metal Compounds*, Springer, Berlin, 1966.
- [17] SAINT-PLUS 2001, Bruker AXS Inc., Madison, WI, 2001.
- [18] G.M. Sheldrick, *Acta Crystallogr. Sect. A* 46 (1990) 467.
- [19] SHELXTL, Bruker AXS Inc., Madison, WI, 2000.
- [20] G.M. Sheldrick, SHELX-97, Universität Göttingen, Germany, 1997.
- [21] DIAMOND—Visual Crystal Structure Information System, Release 3.1d, CRYSTAL IMPACT GbR, Bonn, Germany, 2006.
- [22] A. Nicula, I. Ursu, S. Nistor, *Rev. Roum. Phys.* 10 (1965) 229.
- [23] I. Ghesner, A. Soran, C. Silvestru, J.E. Drake, *Polyhedron* 22 (2003) 3395.
- [24] C. Silvestru, R. Roesler, J.E. Drake, J. Yang, G. Espinoza-Perez, I. Haiduc, *Dalton Trans.* (1998) 73.
- [25] S. Pohl, *Chem. Ber.* 109 (1976) 3122.
- [26] D. Fenske, R. Mattes, J. Loens, K.-F. Tebbe, *Chem. Ber.* 106 (1973) 1139.
- [27] A. Earnshaw, J. Lewis, *J. Chem. Soc.* (1961) 396.
- [28] J.S. Smart, *Effective Field Theories of Magnetism*, W.B. Saunders Comp., Philadelphia and London, 1966.